Evaluation of Free and Hydrostatic Equibiaxial Deformation of Poly(ethylene Terephthalate) by Trirefringence Measurement

JIA Y. GUAN,* RAVI F. SARAF, and ROGER S. PORTER,
Polymer Science and Engineering Department, University of Massachusetts, Amherst, Massachusetts 01003

Synopsis

Understanding the deformation behavior of an amorphous thermoplastic, e.g., poly(ethylene terephthalate) (*a*-PET) and one of semicrystallinity, viz., *i*-PP, can be is of both fundamental and practical importance. Much has been done to study the influence of temperature and strain, but not the influence of deformation conditions on the three-dimensional orientation of many thermoplastic. In this study we consider the incremental effect of hydrostatic pressure and process geometry on strain-induced deformation. *a*-PET has been free drawn (i.e., no hydrostatic pressure) isothermally on a tenter frame device. The hydrostatic, equibiaxial deformation was achieved by a forging process involving squeezing between two circular plates. These two processes have been carried out at a series of deformation rates, with the three-dimensional refractive index measurements having been made on the PET and *i*-PP films using a modified Abbe refractometer, as per Samuels. The reported trirefringence measurement provides a sensitive scale for the planar deformation.

INTRODUCTION

On uniaxial deformation of flexible polymers in solid state, orientation is with the chain axis parallel to the draw direction. This phenomenon is generally true for most polymers,[1] and may be attributed in part to longer relaxation time of the oriented (and strained) chains as compared to the process time (proportional to reciprocal strain rate). For amorphous poly(ethylene terephthalate) (PET), uniaxial deformation induces both chain orientation and crystallization.[2,3] Conversely, the crystallinity drops on draw of highly crystalline (30–50%) (PET).[2] For comparison, a series of experiments were also conducted on isotactic polypropylene. In contrast, crystals of isotactic polypropylene (*i*-PP) uniaxially drawn above glass transition (T_g) orient, but with no significant change in crystallinity.[4]

In this study, amorphous and isotropic PET is biaxially deformed above T_g. The two biaxial flow fields imposed on amorphous PET are Tenter framing ("free drawing") and forging (hydrostatic deformation). The effect of hydrostatic pressure during deformation on the orientation and strain-induced crystallization has thus been studied by comparing the two processes and as a function of rate (i.e., strain rate) and extent of deformation (i.e., draw ratio).

*On leave from: Institute of Chemistry, Academia Sinica, Beijing, China.

Journal of Applied Polymer Science, Vol. 33, 1517–1523 (1987)

CCC 0021-8995/87/051517-07$04.00

Semicrystalline, isotropic *i*-PP has been deformed biaxially by the forging process. A comparison between *i*-PP and PET is made to distinguish the effect of biaxial deformation on precrystallized polymer (*i*-PP) and strain crystallizable polymer (PET). Trirefringence[5] is used to characterize the orientation induced by the deformation field on PET and *i*-PP.

EXPERIMENTAL

Polymers

The sheet of PET used for testing was initially amorphous, as obtained from the Shanghai Chemical Plant in China. The sheet had been extruded and surface quenched on a cold drum. The intrinsic viscosity $[\eta]$, of the films is 0.57 dL/g at 25°C in phenol–tetrachloroethane (50–50). The PET sheets so obtained was shown to be amorphous and isotropic by wide angle X-ray scattering (WAXS), density, and birefringence measurements.

The *i*-PP for study had a melt index of 4.0 corresponding to molecular weight, $\overline{M}_w = 2.9 \times 10^5$ and polydispersity ~ 5. It was supplied by Hercules Inc., as pellets. The sheets (used for forging) were molded under vacuum at 220°C, followed by quenching to 0°C. The sheets so obtained were semicrystalline. The heat of melting measured by DSC was 22.3 cal/g, corresponding to ~ 50% crystallinity. WAXS on the sheet indicates that the crystals are of α-form and the polymer is unoriented.

Sample Preparation: Deformation Process

The biaxial deformation was achieved by two methods: the Tenter framing process[6] and forging.[7] The former deformation corresponds to a 'free drawing," where the polymer is deformed under atmospheric pressure. In the forging process, the sample is subjected to high pressures ($> 10^3$ atm) during deformation. In the Tenter framing process a square sheet of polymer is stretched simultaneously in two directions parallel to sheet surface. Thus a square of dimensions $L_0 \times L_0$ is stretched to a square of size $L \times L$. The biaxial draw ratio is defined as $\lambda = L/L_0$. Forging operation involves a uniaxial compression of polymer sheet parallel to the thickness direction between two circular cylinders. The polymer is stretched in the radial and "hoop" direction as the sheet is compressed. The biaxial draw ratio for the forging process is defined as $\lambda^2 = H/h$, where H is the initial thickness and h is the final thickness.

Trirefringence

The $\lambda \times \lambda$ sheets obtained by Tenter framing and forging processes are characterized for orientation using optical anistropy measurements. The refractive index in the film plane and thickness direction is measured by using an Abbe refractometer with a rotatable light polarizer mounted on the eye piece.[5] To avoid scattering by the surface, 1-bromonaphthalate (of refractive index 1.6576 at 20°C) was used as an immersion fluid. The prisms and the sample were maintained at 25°C by circulating water through the refractometer via constant temperature bath. Figure 1 shows the sample geometry for measurement. The refractive indices N_X, N_Y, and N_Z measured by trirefringence are reported and discussed below.

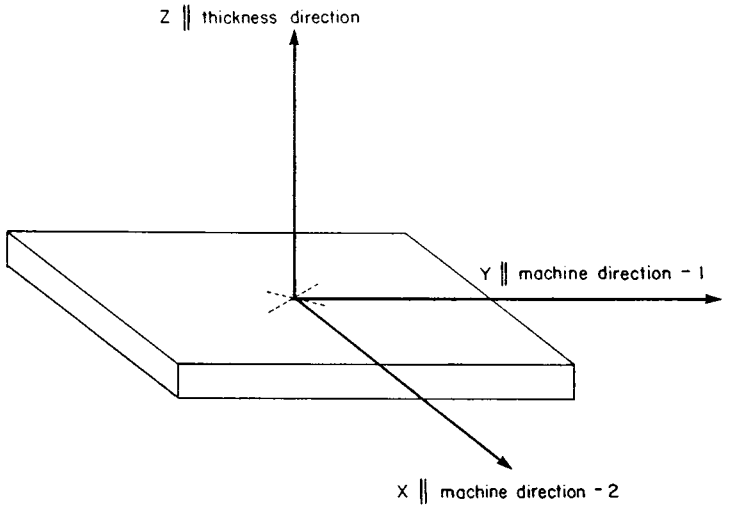

Fig. 1. $X-Y$ plane is parallel to film surface and the Z-axis is parallel to the thickness direction. For the Tenter framing process, the stretching is along the X- and Y-axes. For forging process, the X-axis is equivalent to radial direction and the Y-axis is along the "hoop" direction.

The a-PET was deformed at 90°C by Tenter framing and by forging. The samples were systematically prepared as a function of draw ratio and rate of deformation. The i-PP was forged at 80°C to various draw ratios.

RESULTS AND DISCUSSION

To compare the free drawing deformation (Tenter framing) with hydrostatic deformation (forging), the process conditions (i.e., process temperature, strain rate, and draw ratio) should be made comparable. The process temperature (for PET) in the two processes is 90°C. The strain rate in the two processes is difficult to compare because it changes as the process progresses. Moreover, the trend of strain rate is different for the two processes as shown below.

For the Tenter framing process the tensile strain rate in the two machine directions is given by

$$\dot{\epsilon}_X = \dot{\epsilon}_Y = \dot{\epsilon}_1(t) = W_1/L(t) \tag{1}$$

where, W_1 is the speed of stretching in the two directions X and Y and $L \times L$ are the dimensions of the square sheet at a given time t. For the forging process,[7]

$$\dot{\epsilon}_r = \dot{\epsilon}_\theta \dot{\epsilon}_2(t) = W_2/2h(t) \tag{2}$$

where W_2 is the speed of compression and h is the thickness at given time t. Equations (1) and (2) show that the strain rate in the two processes is time-dependent.

Figures 2 and 3 show the change in refractive indices as a function of initial strain rate (i.e., at $t = 0$) for the two processes (Tenter framing and forging) at draw ratios of 2.5 and 3.0, respectively. Note that the abscissa values of

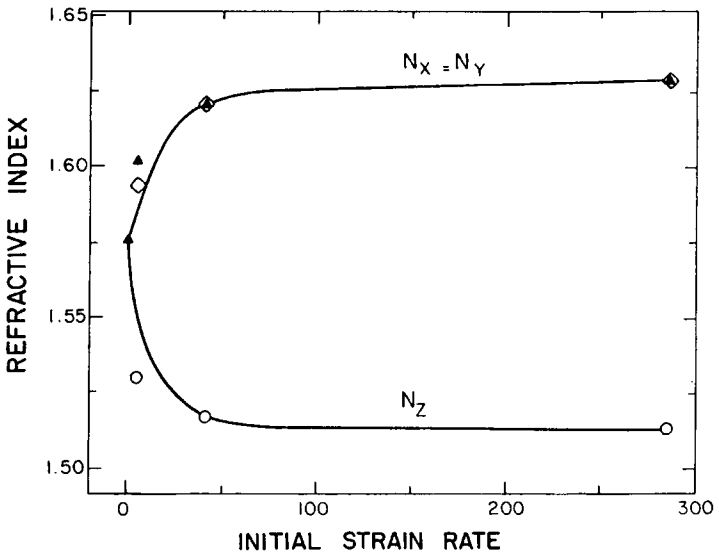

Fig. 2. PET deformed by Tenter framing at 90°C. The initial strain rate is defined as $\dot{\epsilon}_1(0) = W_1/L_0$, where $L_0 = 9.0$ cm.

Figures 2 and 3 are 2-order-of-magnitude different. The dependence of $(N_X - N_Z)$ or $(N_Y - N_Z)$ on initial strain rate for Tenter framing and forging may be rationalized by considering the time dependence of strain rate on the two processes.

Equation (1) indicates that the strain rate decreases with time in the Tenter framing process with the highest strain rate at $\dot{\epsilon}_1(0) = W_1/L_0$. Thus, as the initial strain rate increases, the polymer is subjected to higher strain history

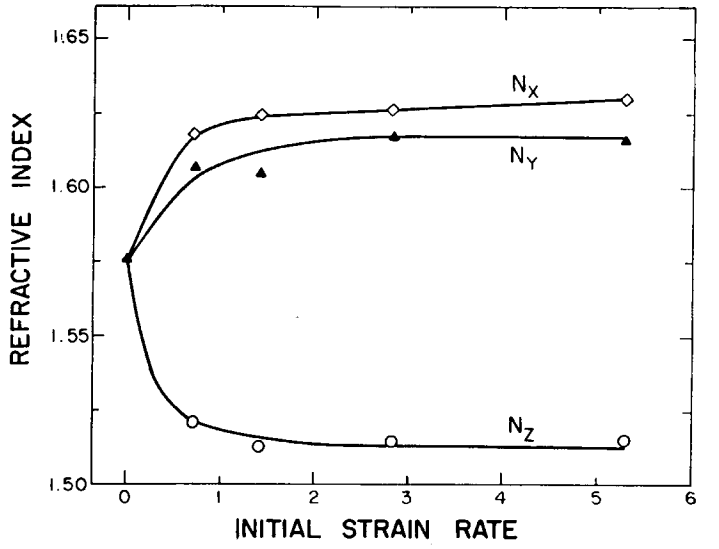

Fig. 3. PET deformed by forging process at 90°C. The initial strain rate is defined as $\dot{\epsilon}_2(0) = W_2/2H$, where $H = 0.36$ cm.

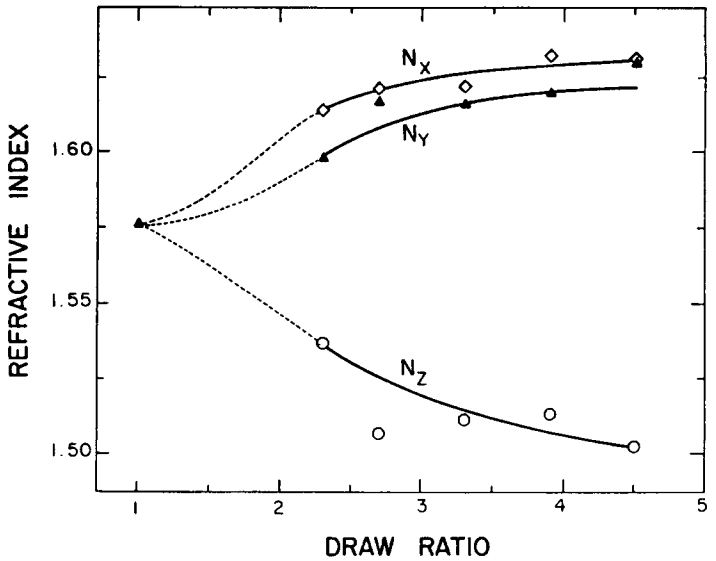

Fig. 4. Deformation of PET at 90°C by forging. The compression speed was 0.51 cm/min, corresponding to an initial strain rate of 0.53 min^{-1}.

for a given final draw ratio (causing higher orientation). Therefore, the initial strain rate is sensitive to the end result. In the forging process the strain rate *increases* with time [see eq. (2)]. Thus, the strain rate at larger times have more effect on the resulting morphology. This implies a weaker dependence of initial strain rate on orientation. Moreover, the plateau should occur at much lower initial strain rate for the forging than Tenter framing (as is evident by comparing Figs. 2 and 3).

The opposite trend in the strain rate with time for the two processes makes the comparison of N_i vs. λ for similar strain history difficult. An appropriate comparison could be possible by equaling the final strain rate of the forging process to the initial strain rate of the Tenter framing process. The functionality of strain rate with time in the two processes is similar, i.e., $\dot{\epsilon} \sim 1/(a + bt)$, where a and b are known constants. For Tenter framing $b = b' > 0$ and for forging $b = b'' < 0$. Now imagine a forging process in negative time (reverse forging process), i.e., the initial strain rate (which in this reversed forging process is the highest strain rate) is equal to $\dot{\epsilon}_1(0)$. As this reversed forging operation progresses, the strain rate decreases as $1/(a - b''t)$, a function similar to the Tenter framing process! For a draw ratio range of 1 to 5 for forging (as shown in Figure 4) a reasonable final strain rate may be calculated at $\lambda = 3$. For $H = 0.48$ cm and $W_2 = 0.51$ cm/min, the final strain rate is given by $W_2/2h = 9W_2/2H = 4.8$/min. Thus, equating the final strain for forging to initial strain, W_1/L_0 for Tenter framing, W_1 can be computed. For $L_0 = 9$ cm a value of ~ 45.0 cm/min for W_1 is obtained. Figures 4 and 5 shows N_i vs. λ for the two processes for comparable strain histories.

For both Tenter framing and forging (see Figs. 2–5) as expected $N_X \approx N_Y$. This suggest orientation symmetric around the Z-direction. Further, N_X and N_Y are greater than N_Z, implying the chain orientation is in the plan normal

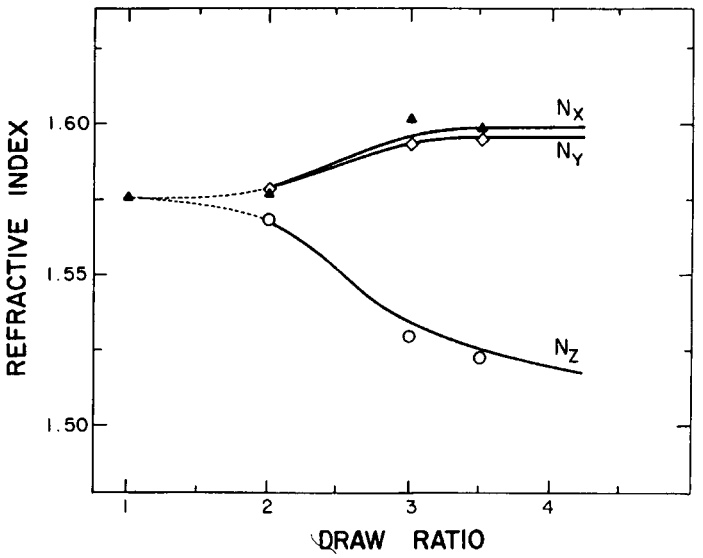

Fig. 5. Deformation of PET at 90°C by Tenter framing. The speed of drawing was 45.0 cm/min, corresponding to initial strain rate of 5.0 min^{-1}.

to Z-axis. Thus, biaxial deformation of PET induces a planar orientation. The orientation increases to a plateau with draw ratio (Figs. 4 and 5).

The hydrostatic deformation induces higher refractive indices and birefringence than free drawing. Moreover, the orientation in the Tenter framing saturates at $\lambda \sim 3.5$ whereas there is a monotonic increase up to $\lambda \gtrsim 4.5$ on forging. The higher refractive indices and corresponding orientation obtained in forging as compared to Tenter framing may be attributed to at least two reasons: (i) The forged sample is more crystalline than the free drawn sample because of the hydrostatic pressure in the former process. Thermal analysis and density measurement confirm higher crystallinity in the forged sample. Thermal analysis reveals that the cold crystallization exotherm ratio of forged sample to free drawn sample is 0.5. (ii) As the polymer orients, the relaxation time of the oriented (strained) chains decreases. Therefore, a process involving increase in strain rate with deformation (as in forging) would be more effective, than a process where the strain rate decreases (as in Tenter framing) or remains constant.

The induced orientation for i-PP during the forging operation is similar to PET (see Fig. 6). This indicates that the orientation of the crystals for preformed crystals (as in i-PP) is similar to strain-induced crystals (as in PET). Moreover, $(N_X - N_Y)$ for i-PP is smaller than for PET (see Figs. 4 and 6). This suggests that planar orientation of i-PP is more ideal than PET. WAXS confirms this result.[8]

The measured birefringence in i-PP is much less than that in PET. This may be related to smaller molecular polarizability in i-PP. The intrinsic birefringence of the crystalline and amorphous regions of i-PP is $\mathring{\Delta}_c = 29.1 \times 10^{-3}$ and $\mathring{\Delta}_a = 60.0 \times 10^{-3}$,[9] respectively; and for PET is $\mathring{\Delta}_c = 220 \times 10^{-3}$ and $\mathring{\Delta}_a = 275 \times 10^{-3}$.[10]

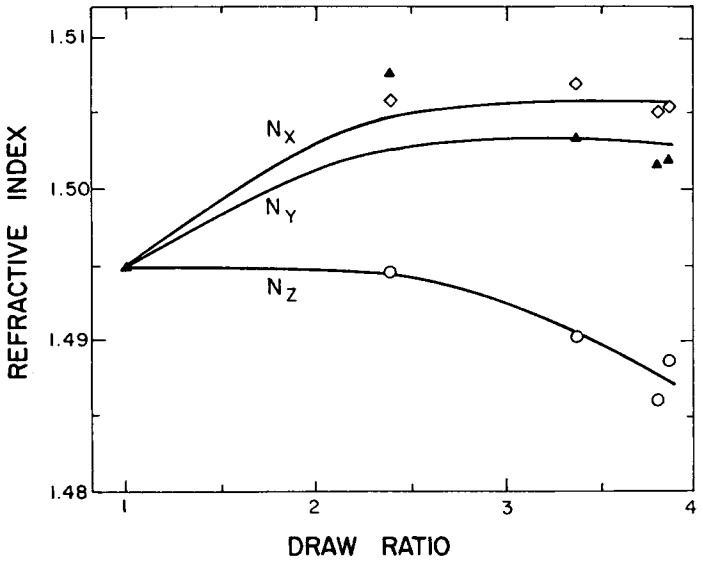

Fig. 6. The change of refractive index of *i*-PP with draw ratio at 80°C for forging process. The compression speed was 0.025 cm/min.

CONCLUSIONS

The essential conclusions drawn from this study are:

(i) Trirefringence measurement provides a sensitive scale for characterizing planar orientation for PET and *i*-PP.

(ii) For PET, hydrostatic biaxial deformation is more efficient than free drawing, with respect, to: (a) more planar orientation in the former process and (b) more induced crystallinity in the former process.

(iii) The texture obtained for *i*-PP is more planar-like than that for PET.

We express appreciation to the Army Research Office for support of this study.

References

1. For example, *Structure and Properties of Oriented Polymers*, I. M. Ward, Ed., Wiley, New York, 1975.
2. J. R. C. Pereira and R. S. Porter, *J. Polym. Sci., Polym. Phys. Ed.*, **21**, 1133 (1983).
3. T. Sun and R. S. Porter, *J. Appl. Polym. Sci.*, **30**, 251 (1985).
4. R. J. Samuels, *Structured Polymer Properties*, Wiley, New York, 1974.
5. R. J. Samuels, *J. Appl. Polym. Sci.*, **26**, 1383 (1981).
6. J. Y. Guan, S. G. Liu, S. L. Wang, and M. Xu, *Polym. Commun.*, **1**, 57 (1984).
7. R. F. Saraf and R. S. Porter, *J. Rheol.*, to appear.
8. R. F. Saraf, J. Y. Guan, and R. S. Porter, to appear.
9. R. J. Samuels, *J. Polym. Sci., A-2*, **6**, 1101 (1968).
10. J. H. Dumpleton, *J. Polym. Sci., A-2*, **6**, 795 (1968).

Received May 27, 1986
Accepted July 19, 1986